2015 IEEE/RSJ International Conference on Intelligent Robots and Systems (IROS)
Congress Center Hamburg
Sept 28 - Oct 2, 2015. Hamburg, Germany

On the Control of Gait Transitions in Quadrupedal Running

Qu Cao, Anthom T. van Rijn and Ioannis Poulakakis

***Abstract*— This paper examines the problem of transitioning between gaits using a sagittal-plane reduced-order model of quadrupedal running, which has compliant elements in its torso and legs. First, periodic motions that correspond to pronking and two variations of bounding are generated. Analysis of the torso pitch motion in these gaits reveals basic differences that determine whether transitions between these gaits can be achieved. This observation is then incorporated in control design to enhance the stability of the generated motions. The domain of attraction of the closed-loop systems is estimated through simulation, showing that transition between pronking and bounding can be realized as a sequence of switchings between fixed points. The results in this work can be regarded as the first step towards synthesizing controllers for gait transitions within template models for quadrupedal running gaits.**

I. Introduction

Quadrupedal animals exhibit various gait patterns, including pronking, trotting, bounding and galloping. Evidence from research in biomechanics suggests that each gait pattern is used over a limited range of speeds and that switching between different gaits occurs at specific speeds [1] to reduce the metabolic cost [1] or the bone stress [2]. Early studies classified quadrupedal gaits with respect to the duration each leg spends on the ground using a footfall formula [3] or a gait diagram [4]. These intuitive observations were later utilized in the development of quadrupedal robots that can switch from trotting to pacing by regulating leg touchdown during flight at low speeds [5].

Subsequent research in robotic legged locomotion concentrated – almost exclusively – on realizing gait transition using neurally inspired controllers [6]–[9], with central pattern generators (CPGs) being a common theme. CPGs are neural networks that produce coordinated patterns of rhythmic activity; for example, different inter-limb coordination patterns can be realized with simple input signals and without rhythmic feedback as explained in [10]. By tuning the phase difference between the legs, transitions between walking and trotting have been realized in several quadrupedal robots [6]–[9]. However, the generated motions are at low speeds and not highly dynamic.

This work is supported in part by NSF grant CMMI-1130372 and ARL contract W911NF-12-1-0117, and by the European Union (European Lifelong Learning of the National Strategic Reference Framework (NSRF)) – Research Funding Program: ARISTEIA: Reinforcement of the interdisciplinary and/ or inter-institutional research and innovation.

Q. Cao and I. Poulakakis are with the Department of Mechanical Engineering, University of Delaware, Newark, DE 19716, USA; e-mail: {caoqu, poulakas}@udel.edu.

A. T. van Rijn is with the Department of Mechanical Engineering, Eindhoven University of Technology, Eindhoven, The Netherlands; e-mail: a.t.v.rijn@student.tue.nl.

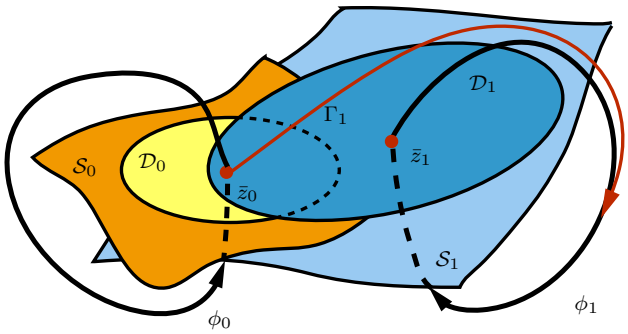

Fig. 1. A conceptual illustration of the transition between two different limit cycles, i.e., ϕ_0 and ϕ_1, which in legged locomotion could correspond to periodic motions of different gaits, for instance, pronking and bounding in this study. $\mathcal{S}_0$ and $\mathcal{S}_1$ are the Poincaré sections of ϕ_0 and ϕ_1, and $\bar{z}_0$ and $\bar{z}_1$ are the corresponding fixed points. $\mathcal{D}_0$ and $\mathcal{D}_1$ are the domain of attractions at the Poincaré sections for ϕ_0 and ϕ_1, respectively.

In this paper, we focus on investigating gait transitions in quadrupedal running using a reduced-order model – a "template" in the terminology used in [11] – which can capture the dominant features of different gaits without delving into the fine structural characteristics of a robot (or an animal). A series of template models of different morphologies have been proposed to study symmetric quadrupedal running gaits in a reductive setting [12]–[16]. However, the majority of these models study gaits *individually*; a model can perform one or several types of gaits, but no transitions between these gaits are examined. In this work, however, we turn our attention to the feasibility of gait transitions by analyzing the dynamic and the stability properties of different dynamic quadrupedal gaits. Our objective is to provide feedback controllers that guarantee stable switching from a source to a targeted gait pattern.

In more detail, gait transition is formulated as a problem of switching between limit cycles as is conceptually illustrated in Fig. 1. The limit cycles, ϕ_0 and ϕ_1, represent periodic motions corresponding to different gaits; in this study, we restrict our attention to pronking and bounding. To characterize stability, the method of Poincaré is used, resulting in two discrete-time mappings $\mathcal{P}_0$ and $\mathcal{P}_1$ and the corresponding fixed points $\bar{z}_0$ and $\bar{z}_1$. Assuming the two limit cycles are stabilized under the influence of the controllers Γ_0 and Γ_1, respectively, the domain of attraction of the limit cycles on the Poincaré sections $\mathcal{S}_0$ and $\mathcal{S}_1$ can be estimated as $\mathcal{D}_0$ and $\mathcal{D}_1$. By examining the relationship between the estimated domains of attraction and the fixed points, feasible transitions can be determined. For instance, as shown in Fig. 1, if $\bar{z}_0$ is within the domain of attraction of ϕ_1 at the Poincaré section, then by employing the controller Γ_1, the states starting from

$\bar{z}_0$ will eventually converge to the orbit ϕ_1, i.e., switch to $\bar{z}_1$. Mathematically, if $\bar{z}_0 \in \mathcal{D}_1$, then $\bar{z}_0 \xrightarrow{\Gamma_1} \bar{z}_1$. Furthermore, if $\bar{z}_1 \in \mathcal{D}_0$, then two-way transitions can be realized between the two gaits, i.e., $\bar{z}_0 \underset{\Gamma_0}{\overset{\Gamma_1}{\longleftrightarrow}} \bar{z}_1$.

II. Model and Gaits

A. Sagittal-plane quadrupedal model

Since both pronking and bounding are symmetric gaits, gait transition can be studied using a reductive model in the sagittal plane; see Fig. 2. The torso of the model consists of two identical rigid bodies; one represents its posterior and the other its anterior part. The two rigid bodies are connected through a rotational spring to introduce flexibility in the torso. The anterior and the posterior legs are assumed to be massless springs and their contact with the ground is modeled as an unactuated, frictionless pin joint. The mechanical parameters of the model can be found in [15] and are omitted here.

B. Gait description

In the pronking gait, shown in Fig. 3(a), both the anterior and the posterior legs touch and leave the ground in unison. In the bounding gait, shown in Fig. 3(b), two variations in the footfall pattern are considered. In the first variation, which is referred as *bounding with double stance*, the posterior leg touchdown occurs directly after the anterior leg touchdown, thus there is a part of the cycle where both legs are in stance. In the second variation, which is referred as *bounding without double stance*, the posterior leg touchdown happens after the anterior leg liftoff, thus the posterior and anterior stance phases are separated by a double flight phase. For both pronking and bounding, depending on the state of the legs – stance or flight – we distinguish the following phases: the double flight phase, denoted by "f", in which both legs are in the air; the stance-posterior phase, denoted by "sp", when only the posterior leg is on the ground; the stance-anterior phase, denoted by "sa", when only the anterior leg is on the ground; and the double stance phase, denoted by "sd", in which both legs are in contact with the ground.

C. Dynamics in continuous time

For the anterior and the posterior stance phases, i.e., $i \in \{\mathrm{sp}, \mathrm{sa}\}$, the configuration space Q_i can be parameterized

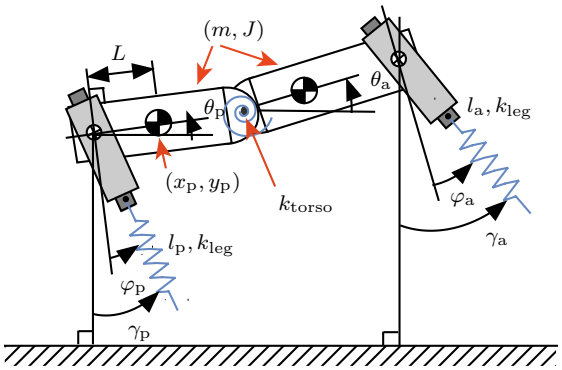

Fig. 2. A sagittal-plane quadrupedal model with a flexible segmented torso.

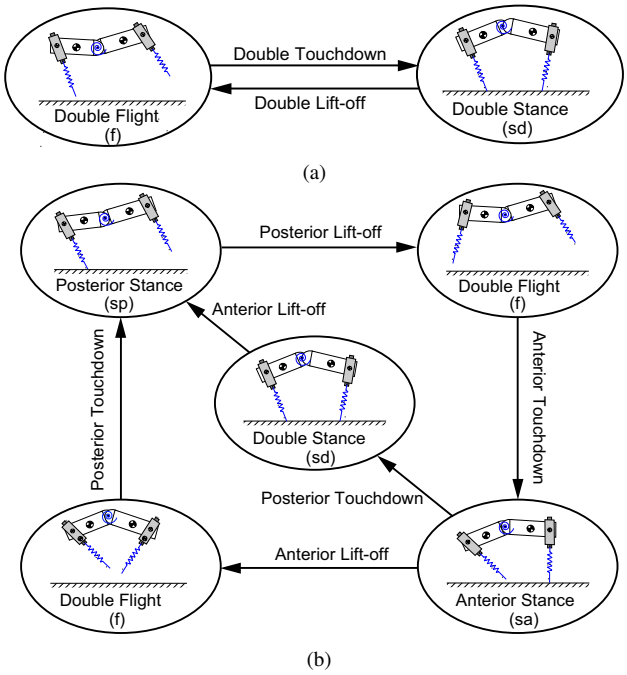

Fig. 3. (a) Pronking; (b) Two variations of bounding.

by the length $l_\mathrm{a}, l_\mathrm{p} \in \mathbb{R}$ of the leg in contact with the ground and its relative angle $\varphi_\mathrm{a}, \varphi_\mathrm{p} \in \mathbb{S}^1$ with respect to the torso, together with the pitch angles $(\theta_\mathrm{p}, \theta_\mathrm{a}) \in \mathbb{S}^2$ of the posterior and the anterior parts of the torso, respectively. The configuration space Q_i of the double stance phase, i.e., when $i = \mathrm{sd}$, is selected as in the stance-posterior phase. For the flight phase, i.e., when $i = \mathrm{f}$, the configuration space Q_i can be parameterized by the Cartesian coordinates $(x_\mathrm{p}, y_\mathrm{p}) \in \mathbb{R}^2$ of the center of mass of the posterior part of the torso and the pitch angles $(\theta_\mathrm{p}, \theta_\mathrm{a}) \in \mathbb{S}^2$ of the two segments of the torso. In summary,

$$q_i := \begin{cases} (l_\mathrm{p}, \varphi_\mathrm{p}, \theta_\mathrm{p}, \theta_\mathrm{a})' \in Q_i & \text{for } i \in \{\mathrm{sp}, \mathrm{sa}\}, \\ (l_\mathrm{a}, \varphi_\mathrm{a}, \theta_\mathrm{p}, \theta_\mathrm{a})' \in Q_i & \text{for } i = \mathrm{sd}, \\ (x_\mathrm{p}, y_\mathrm{p}, \theta_\mathrm{p}, \theta_\mathrm{a})' \in Q_i & \text{for } i = \mathrm{f}. \end{cases} \tag{1}$$

Through the method of Lagrange, the dynamics of the model in each phase can be written in state-space form as

$$\dot{x}_i = f_i(x_i), \tag{2}$$

evolving in $TQ_i := \{x_i := (q_i', \dot{q}_i')' \mid q_i \in Q_i,\ \dot{q}_i \in \mathbb{R}^4\}$. Note that at this stage, no actuation is employed in the system; the system is passive and energy conservative.

D. Event-based transitions

Phase-to-phase transitions occur according to Fig. 3, and are triggered by leg touchdown and liftoff events. The flight phase terminates when the vertical distance between the toe of either the posterior or the anterior leg and the ground becomes zero. To realize this condition, the flight state vector x_f is augmented with the parameter array $\alpha_\mathrm{f} = (\gamma_\mathrm{p}^\mathrm{td}, \gamma_\mathrm{a}^\mathrm{td}) \in \mathcal{A}_\mathrm{f}$ containing the absolute touchdown angles of the posterior and the anterior legs; see Fig. 2. In addition, due to the assumption of negligible leg mass, transition from stance to flight occurs when the leg spring obtains its natural length.

E. Hybrid Dynamics

The dynamics of bounding and pronking can be described by concatenating the continuous-time phases according to the sequence in Fig. 3. To generate periodic motions, the Poincaré method is used. The Poincaré section is taken at the apex height in the flight phase following the anterior stance when the vertical velocity of the spinal joint becomes zero; that is,

$$\mathcal{S}_{\text{apex}} := \left\{ (x_{\text{f}}, \alpha_{\text{f}}) \in \mathcal{X}_{\text{f}} \mid \dot{y}_{\text{p}} + L\dot{\theta}_{\text{p}} \cos\theta_{\text{p}} = 0 \right\}, \quad (3)$$

where $\mathcal{X}_{\text{f}} := TQ_{\text{f}} \times \mathcal{A}_{\text{f}}$. By projecting out the monotonically increasing quantity x_{p} from the flight states x_{f} and substituting $\dot{y}_{\text{p}}$ through the condition defining $\mathcal{S}_{\text{apex}}$, the (reduced) Poincaré map $\mathcal{P} : \tilde{\mathcal{S}}_{\text{apex}} \to \tilde{\mathcal{S}}_{\text{apex}}$ can be defined as

$$z_{\text{f}}[k+1] = \mathcal{P}\left(z_{\text{f}}[k], \alpha_{\text{f}}[k]\right), \quad (4)$$

where $z_{\text{f}} := (y_{\text{p}}, \theta_{\text{p}}, \theta_{\text{a}}, \dot{x}_{\text{p}}, \dot{\theta}_{\text{p}}, \dot{\theta}_{\text{a}})'$. The problem of generating periodic motions then reduces to solving the equation

$$z_{\text{f}} - \mathcal{P}(z_{\text{f}}, \alpha_{\text{f}}) = 0 \quad (5)$$

for physically reasonable values of touchdown angles α_{f}.

The local stability of the periodic motions can be examined by linearizing the Poincaré return map at a fixed point $(\bar{z}_{\text{f}}, \bar{\alpha}_{\text{f}})$ to obtain

$$\Delta z_{\text{f}}[k+1] = A_1 \Delta z_{\text{f}}[k] + B_1 \Delta\alpha_{\text{f}}[k], \quad (6)$$

where $A_1 = \partial\mathcal{P}/\partial z_{\text{f}}|_{z_{\text{f}}=\bar{z}_{\text{f}}, \alpha_{\text{f}}=\bar{\alpha}_{\text{f}}}$, $B_1 = \partial\mathcal{P}/\partial\alpha_{\text{f}}|_{z_{\text{f}}=\bar{z}_{\text{f}}, \alpha_{\text{f}}=\bar{\alpha}_{\text{f}}}$ and $\Delta z_{\text{f}} = z_{\text{f}} - \bar{z}_{\text{f}}$, $\Delta\alpha_{\text{f}} = \alpha_{\text{f}} - \bar{\alpha}_{\text{f}}$. If the spectral radius of A_1 is less than one, then the periodic motion is stable; note that for the energy-conservative models discussed above, there will always be one eigenvalue located at one.

III. Passively Generated Motions

A large number of passively generated fixed points corresponding to the gaits of Fig. 3 are computed following the procedure outlined in Section II-E. All the fixed points exhibit certain symmetry properties as observed in [15], which will be useful in designing transition controllers. In more detail, for both pronking and bounding, $\theta_{\text{p}} = -\theta_{\text{a}}$ and $\dot{\theta}_{\text{p}} = \dot{\theta}_{\text{a}}$ at the apex height. In particular, the pronking motion has zero pitch velocity at this instant, i.e., $\dot{\theta}_{\text{p}} = \dot{\theta}_{\text{a}} = 0$.

These symmetry properties facilitate the investigation of the states that distinguish the two gaits at the Poincaré section. Figure 4 shows the apex height, the posterior pitch angle and the posterior pitch rate of the fixed points corresponding to the pronking and the two variations of bounding. It can be seen that these three types of motions can be distinguished by the pitch rate of the posterior part of the torso; pronking has zero pitch rate, bounding with double stance has relatively small pitch rate magnitude (< 2.5 rad/s) and bounding without double stance exhibits larger values of pitch rate (in the range $[2.5 \text{ rad/s}, 5 \text{ rad/s}]$).

The significant difference in the pitch rate shown in Fig. 4(c) clearly demonstrates the natural separation in the dynamics of different gaits, and reveals a major challenge in achieving gait transition. In the context of transitioning from from pronking to bounding without double stance, the model needs to experience a drastic perturbation in the torso oscillation dynamics, which can easily destabilize the motion. In other words, following the definition in Section I, if bounding without double stance is regarded as the target and pronking as the starting limit cycle, to guarantee convergence, the domain of attraction of the bounding limit cycle should be large enough to include the states of the pronking motion at the Poincaré section. However, the model in its passive and conservative form is limited in rejecting disturbances and all the fixed points computed are not stable. As a result, transitioning from pronking to bounding calls for control laws that stabilize the gaits and ensures that the domain of attraction of the target gait is sufficiently large.

IV. Feedback Control

In this section, a controller that utilizes actuation at the torso joint is developed to stabilize the pronking and bounding motions computed in Section III. A similar controller has been proposed in our previous work [17].

A. An extended gait description

To enhance stability, the model is allowed to go through additional phases beyond the nominal phase sequence as it converges to the target motion; see Fig. 5. For example, in the nominal pronking motion, both the anterior and posterior legs touch and leave the ground in unison with the same touchdown angle. However, when the motion is disturbed

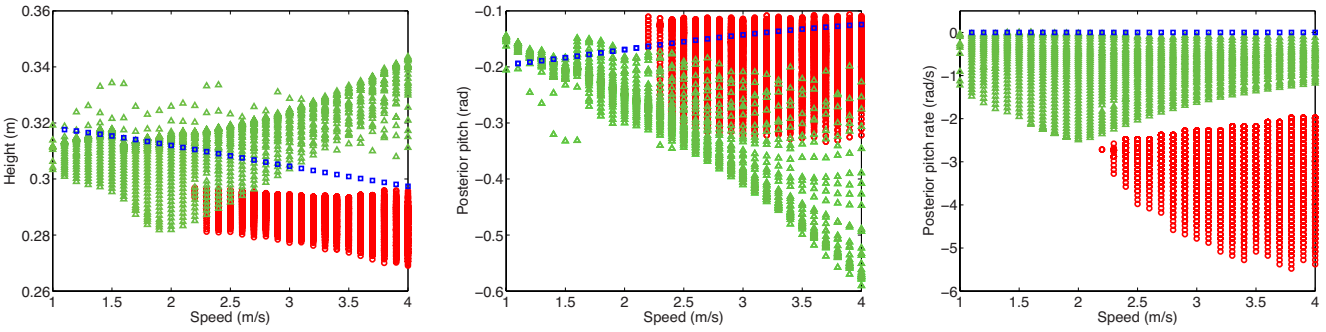

(a) (b) (c)

Fig. 4. The apex height (a), posterior pitch angle (b) and posterioe pitch rate (c) of the fixed points corresponding to pronking (blue square), bounding without double stance (green triangle) and bounding with double stance (red circle) at speed $[1, 4]$m/s.

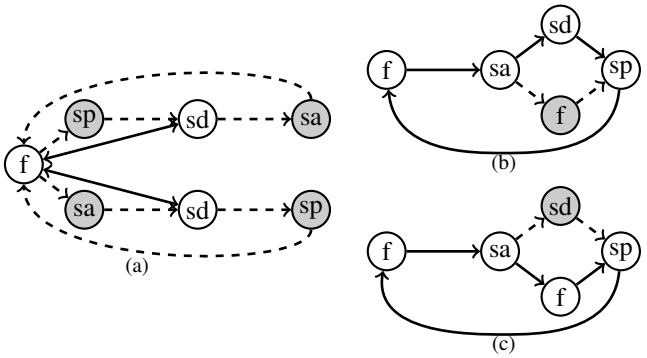

Fig. 5. Extended description of the gaits in the presence of perturbation for pronking (a), bounding with double stance (b) and bounding without double stance (c). The shaded phases are the augmented phases and the dotted lines represent the possible evolution in presence of perturbation.

during flight – e.g., when the anterior pitch angle increases – then determining the touchdown angles $\alpha_{\rm f}$ that result in simultaneous touchdown and liftoff requires numerically solving the dynamics of the double stance phase. To avoid such cumbersome computation, the model is allowed to enter either posterior stance or anterior stance before entering the double stance phase; see Fig. 5(a). Under the control action, the duration of these two augmented phases gradually decreases to zero, resulting in the nominal periodic motion. In Fig. 5(b) and 5(c), the double flight and double stance phases are augmented after the anterior stance for bounding with and without double stance, respectively.

B. Hybrid controller

The hybrid controller introduces control action on two levels. In continuous time, holonomic constraints are imposed to the system to coordinate – according to a passively generated motion – the torso's flexion-extension oscillations with the leg's motion during stance. In discrete time, the touchdown angles are updated at apex through a linear quadratic regulator.

1) Continuous-time control: To enable the development of non-conservative corrective forces, the model in Fig. 2 is modified to incorporate one actuator at the torso joint in parallel with the torso spring. With this modification, the dynamics in each phase $i \in \{\rm f, sp, sa, sd\}$ becomes

$$\dot{x}_i = f_i(x_i) + g_i(x_i)u_i \tag{7}$$

where u_i is the input torque at the torso joint.

In the flight phase, the input is zero, i.e., $u_{\rm f} = 0$ and in the stance phases, i.e., $i \in \{\rm sp, sa, sd\}$, we define the output

$$y_i := h_i(q_i) := (\theta_{\rm p} - \theta_{\rm a}) - h^{\rm d}_{{\rm P},i}(q_i) \tag{8}$$

where $h^{\rm d}_{{\rm P},i}(q_i)$ is the desired evolution of the relative pitch angle $\theta_{\rm p} - \theta_{\rm a}$. Note that in (8), $h_i(q_i)$ is a function of the configuration variables instead of time, and therefore can be interpreted as a (virtual) holonomic constraint. This constraint is imposed on the system through a PD controller:

$$u_i = K_{{\rm P},i}y_i + K_{{\rm D},i}\dot{y}_i, \tag{9}$$

where $K_{{\rm P},i}$ and $K_{{\rm D},i}$ are selected gains.

In (8), the desired evolution $h^{\rm d}_{{\rm P},i}(q_i)$ is determined by a fifth-degree polynomial parameterized by the leg angles that is fitted to the passively generated motions as in [17]; i.e.,

$$h^{\rm d}_{{\rm P},i}(q_i) = \sum_{k=0}^{5} \beta_{i,k} s_i^k(q_i), \tag{10}$$

where $\beta_i = \{\beta_{i,k}\}_{k=0,\dots,5}$ are the corresponding coefficients and s_i is defined as

$$s_i(q_i) := \frac{\gamma^{\max} - \gamma(q_i)}{\gamma^{\max} - \gamma^{\min}} \tag{11}$$

where

$$\gamma(q_i) := \begin{cases} \gamma_{\rm p}, & \text{for } i \in \{\rm sp, sd\}, \\ \gamma_{\rm a}, & \text{for } i = \rm sa, \end{cases} \tag{12}$$

and $\gamma^{\min}$ and $\gamma^{\max}$ are the minimum and maximum values of γ in the corresponding stance phase of the nominal motion.

With the continuous-time control action, the closed loop Poincaré map (4) becomes

$$z_{\rm f}[k+1] = \mathcal{P}_1^{\rm cl}\left(z_{\rm f}[k], \alpha_{\rm f}[k]\right), \tag{13}$$

and its linearization takes the form

$$\Delta z_{\rm f}[k+1] = A_2 \Delta z_{\rm f}[k] + B_2 \Delta \alpha_{\rm f}[k] \ , \tag{14}$$

where A_2 and B_2 are the Jacobian matrices of $\mathcal{P}_1^{\rm cl}$ with respect to $z_{\rm f}$ and $\alpha_{\rm f}$ evaluated at a fixed point, respectively.

2) Discrete-time control: A discrete linear quadratic regulator is employed to place the legs during flight based on feedback of the states at the Poincaré section to minimize the quadratic cost function

$$\begin{aligned} J(z_{\rm f}, \alpha_{\rm f}) = \sum_{k=1}^{\infty} & (z_{\rm f}[k] - \bar{z}_{\rm f})' Q (z_{\rm f}[k] - \bar{z}_{\rm f}) + \\ & (\alpha_{\rm f}[k] - \bar{\alpha}_{\rm f})' R (\alpha_{\rm f}[k] - \bar{\alpha}_{\rm f}) \end{aligned} \tag{15}$$

where $\bar{z}_{\rm f}$ and $\bar{\alpha}_{\rm f}$ represent the nominal states and touchdown angles, and Q, R are positive definite matrices. It can be shown that the optimal cost-to-go, J^*, is given by

$$J^*(z_{\rm f}) = (z_{\rm f}[k] - \bar{z}_{\rm f})' S (z_{\rm f}[k] - \bar{z}_{\rm f}) \tag{16}$$

where S is the infinite horizon solution of the associated discrete-time Riccati equation. The optimal feedback policy is then given by

$$\alpha_{\rm f}[k] = \bar{\alpha}_{\rm f} - K(z_{\rm f}[k] - \bar{z}_{\rm f}) \tag{17}$$

where $K = (B_2' S B_2 + R)^{-1}(B_2' S A_2)$ and A_2, B_2 have been defined in (14).

3) Closed-loop system with hybrid control: With the hybrid control action, the closed-loop form of the Poincaré map (13) can be written as

$$\begin{aligned} z_{\rm f}[k+1] &= \mathcal{P}_1^{\rm cl}\left(z_{\rm f}[k], \bar{\alpha}_{\rm f} - K(z_{\rm f}[k] - \bar{z}_{\rm f})\right) \\ &= \mathcal{P}_2^{\rm cl}\left(z_{\rm f}[k]\right) \end{aligned} \tag{18}$$

Defining $\beta := \{\beta_{\rm sp}, \beta_{\rm sa}\}$, then the parameters that characterize a locally stable gait are given in

$$\Gamma := \{\bar{z}_{\rm f}, \bar{\alpha}_{\rm f}, \gamma^{\max}, \gamma^{\min}, \beta, K\} \tag{19}$$

that contains the information of the nominal motion as well as the coefficients and the matrix used in controller design.

V. Gait Transition

As an example of gait transitions, this section examines switching between pronking and bounding without double stance. First, the strategy of estimating the domain of attraction of the closed-loop system is introduced. Then, the transition will be illustrated as a sequence of switchings among fixed points with the bounding with double stance as an intermediate gait.

A. Estimation of domain of attraction

Computing the exact domain of attraction for nonlinear systems is generally intractable, even at low dimensions. An alternative is to estimate the domain of attraction using Lyapunov's method [18]. A function $V(z_{\mathrm{f}})$ is a valid Lyapunov function for the discrete-time system (18) if $V(z_{\mathrm{f}})$ is positive definite and $V(z_{\mathrm{f}}[k+1])-V(z_{\mathrm{f}}[k]) < 0$ in a bounded domain $\mathcal{B}$. Then, a subset of the domain of attraction of a fixed point on the (reduced) Poincaré section $\tilde{\mathcal{S}}_{\mathrm{apex}}$ can found as

$$\mathcal{B}(\rho) := \{z_{\mathrm{f}} \in \tilde{\mathcal{S}}_{\mathrm{apex}} \mid 0 \leq V(z_{\mathrm{f}}) \leq \rho\} \tag{20}$$

where ρ is a positive scalar. Note that the linear optimal cost-to-go function (16) is already a Lyapunov function for the nonlinear system (18) since S is positive definite. Thus by defining $V(z_{\mathrm{f}}) := J^*(z_{\mathrm{f}})$, the problem of estimating the domain of attraction on $\tilde{\mathcal{S}}_{\mathrm{apex}}$ reduces to

$$\begin{aligned} &\max\ \rho \\ &\text{s.t}\ \ \forall z_{\mathrm{f}} \in \mathcal{B}(\rho), J^*(z_{\mathrm{f}}[k+1]) - J^*(z_{\mathrm{f}}[k]) < 0 \end{aligned} \tag{21}$$

which can be solved using the sum-of-squares (SOS) method [19]. However, due to the error incurred in approximating the closed-loop Poincaré map $\mathcal{P}_2^{\mathrm{cl}}$ of (18) by its second-order Taylor expansions, the analytically guaranteed estimate of the domain of attraction for (18) is rather conservative. As an alternative, a simulation-based method is used to provide a more complete estimate. Given the target fixed point $\bar{z}_{\mathrm{f},0}$, other fixed points $\bar{z}_{\mathrm{f},i}, i \in \{1,2,3,...\}$ are taken as initial conditions and the hybrid controller associated with the target fixed point Γ_0 is applied. If after 15 strides the error of the states from the nominal values is less than 5%, then the fixed point $\bar{z}_{\mathrm{f},i}$ is regarded as being in the domain of attraction of $\bar{z}_{\mathrm{f},0}$, i.e., $\bar{z}_{\mathrm{f},i} \in \mathcal{D}_0$. Figure 6 shows that – for the bounding gait with double stance – a large number of fixed point (black) lie inside the domain of attraction of the target fixed point (blue). On the other hand, the sum-of-square algorithm, in its current implementation, only verifies a very small portion (red). Improving the SOS method to obtain a more complete characterization of the domain of attraction is currently under investigation.

B. Transitions between pronking and bounding

Without loss of generality, we explore gait transitions between pronking and bounding at speed $2.4\mathrm{m/s}$; see Fig. 7. Note that $\bar{z}_{\mathrm{f},0}$ and $\bar{z}_{\mathrm{f},1}$ correspond to the pronking motion and the bounding motion without double stance, respectively. It can be easily checked through the simulation-based method described in Section V-A that direct transition cannot be realized in either direction – i.e., $\bar{z}_{\mathrm{f},0} \notin \mathcal{D}_1$ and $\bar{z}_{\mathrm{f},1} \notin \mathcal{D}_0$ –

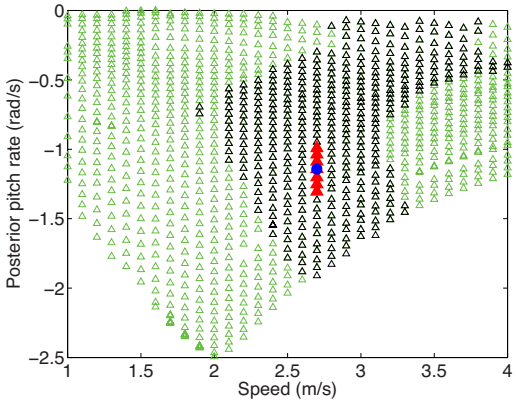

Fig. 6. Fixed points that can be driven to a target fixed point (blue) within the double-stance bounding gait. The black points are tested using simulation method while the red points are predicted by the SOS algorithm.

which confirms the predictions of Fig. 4(c). To bridge this gap, bounding with double stance serves as intermediate gait between the initial and target gaits.

With reference to Fig. 4(c), we first examine the transition between the two variations of bounding, which exhibits an asymmetry. The bounding gait without double stance can converge to a large number of fixed points corresponding to the bounding gait with double stance (enclosed by solid red). On the contrary, only a few of bounding motions with double stance (enclosed by dotted red) can switch to the bounding gait without double stance and they all have pitch velocity close to the bounding without double stance; see Fig. 4(c).

The transition between bounding with double stance and pronking exhibits a similar behavior; the pronking motion can switch to a large range of bounding motions (enclosed by solid blue), but – in the opposite direction – only a limited number of bounding fixed points (enclosed by dotted blue) are within the domain of attraction of the pronking motion. In addition, the magnitude of the pitch velocity of these bounding motions is approximately zero, which describes the pitch velocity of the pronking motion.

Given the aforementioned intermediate transitions, the task of switching between pronking and bounding without double stance reduces to the transition between two fixed points within the bounding gait with double stance; i.e., $\bar{z}_{\mathrm{f},2}$ and $\bar{z}_{\mathrm{f},3}$ in Fig. 4(c). Noticing that $\bar{z}_{\mathrm{f},2} \notin \mathcal{D}_3$ and $\bar{z}_{\mathrm{f},3} \notin \mathcal{D}_2$, two more intermediate fixed points $\bar{z}_{\mathrm{f},4}$ and $\bar{z}_{\mathrm{f},5}$ are introduced to complete the transition path, which is

$$\bar{z}_{\mathrm{f},0} \underset{\Gamma_0}{\overset{\Gamma_2}{\longleftrightarrow}} \bar{z}_{\mathrm{f},2} \underset{\Gamma_2}{\overset{\Gamma_5}{\longleftrightarrow}} \bar{z}_{\mathrm{f},5} \underset{\Gamma_5}{\overset{\Gamma_4}{\longleftrightarrow}} \bar{z}_{\mathrm{f},4} \underset{\Gamma_4}{\overset{\Gamma_3}{\longleftrightarrow}} \bar{z}_{\mathrm{f},3} \underset{\Gamma_3}{\overset{\Gamma_1}{\longleftrightarrow}} \bar{z}_{\mathrm{f},1} \tag{22}$$

In Fig. 7, the arrows illustrate the two-way transition between pronking and bounding without double stance. In both directions, the transitions can be completed within 50 strides. It should be mentioned that when only one-way transition is considered, a "shortcut" route can be selected to decrease the number of strides required. For instance, switching from bounding without double stance to pronking only needs less than 20 strides via the route $\bar{z}_{\mathrm{f},0} \xrightarrow{\Gamma_3} \bar{z}_{\mathrm{f},3} \xrightarrow{\Gamma_1} \bar{z}_{\mathrm{f},1}$.

Finally, we remark that the proposed transition strategy can be used to enlarge the domain of attraction of the fixed

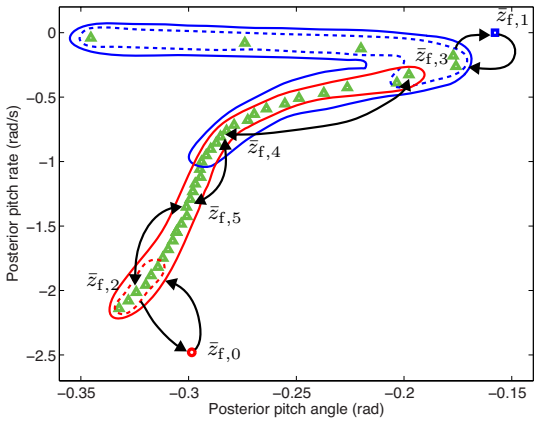

Fig. 7. The transition between pronking and bounding without double stance in the $(\theta_{\mathrm{p}}, \dot{\theta}_{\mathrm{p}})$ section. The blue square, red circle and green triangles represent the fixed points corresponding to the target pronking, the target bounding without double stance and the bounding with double stance, respectively. The black arrows show one of the transition routes.

points, drastically improving the capability of the system to reject large perturbations. For instance, when the bounding motion $\bar{z}_{\mathrm{f},0}$ is perturbed outside of its original domain of attraction, the states cannot converge back to their nominal values by mere use of the corresponding controller Γ_0. Yet, if the states are located within the domain of attraction of $\bar{z}_{\mathrm{f},5}$, then Fig. 7 shows that implementing Γ_5, Γ_2 and Γ_0 sequentially realizes convergence to $\bar{z}_{\mathrm{f},0}$. In fact, the two-way transition sequence (22) indicates that any states located within the domain of attraction of one of the fixed points in the sequence can be driven to any other fixed point in the sequence by suitably switching the parameters of the controller in (19). This way, the domain of attraction of each fixed point is expanded as the union of the domains of attraction of all the fixed points in the sequence; i.e., $\bigcup_{i=0,1,\ldots 5} \mathcal{D}_i$. This expansion can be conducted iteratively – in a fashion similar to the LQR-tree algorithm [20] – thereby significantly enhancing motion stability.

VI. Conclusions and Future Work

In this paper, the gait transition between pronking and bounding is studied using a reduced-order quadrupedal model. A large number of cyclic motions are generated passively, showing that the two gaits are distinguished by the rate of torso oscillation at the apex height. To stabilize the passively generated motions, a hybrid controller that coordinates the torso oscillation with respect to the leg movement during stance and updates the touchdown angles at the apex height is developed. The domain of attraction of the closed-loop system is estimated in order to search for possible transitions between different fixed points. By using bounding with double stance as an intermediate gait, two-way transitions can be realized between pronking and bounding without double stance.

Future work will focus on two aspects. First, the implementation of the sum-of-squares technique in estimating the domain of attraction will be improved so that transitions can be determined in a guaranteed way, without extensively relying on simulations. Second, the transition strategy will be extended to involve more gaits, such as trotting and galloping in order to create more complex running behaviors.

References

[1] D. F. Hoyt and C. R. Taylor, "Gait and the energetics of locomotion in horses." *Nature*, vol. 292, pp. 239 – 240, 1981.

[2] A. A. Biewener and C. R. Taylor, "Bone strain: a determinant of gait and speed?" *Journal of Experimental Biology*, vol. 123, no. 1, pp. 383–400, 1986.

[3] E. Muybridge, *Animals in Motion*. New York: Courier Dover Publications, 1957.

[4] M. Hildebrand, "The quadrupedal gaits of vertebrates: The timing of leg movements relates to balance, body shape, agility, speed, and energy expenditure," *BioScience*, vol. 39, no. 11, pp. 766–775, 1989.

[5] M. H. Raibert, "Trotting, pacing and bounding by a quadruped robots," *Journal of Biomechanics*, vol. 23, pp. 79–98, 1990, suppl. 1.

[6] K. Tsujita, K. Tsuchiya, and A. Onat, "Adaptive gait pattern control of a quadruped locomotion robot," in *Proceedings of the IEEE/RSJ International Conference on Intelligent Robots and Systems*, vol. 4, Maui, HI, Oct. 2001, pp. 2318–2325.

[7] K. Tsujita, T. Kobayashi, T. Inoura, and T. Masuda, "Gait transition by tuning muscle tones using pneumatic actuators in quadruped locomotion," in *Proceedings of the IEEE/RSJ International Conference on Intelligent Robots and Systems*, Nice, France, Sep. 2008, pp. 2453–2458.

[8] C. P. Santos and V. Matos, "Gait transition and modulation in a quadruped robot: A brainstem-like modulation approach," *Robotics and Autonomous Systems*, vol. 59, no. 9, pp. 620–634, 2011.

[9] S. Aoi, D. Katayama, S. Fujiki, N. Tomita, T. Funato, T. Yamashita, K. Senda, and K. Tsuchiya, "A stability-based mechanism for hysteresis in the walk–trot transition in quadruped locomotion," *Journal of The Royal Society Interface*, vol. 10, no. 81, p. 20120908, 2013.

[10] A. J. Ijspeert, "Central pattern generators for locomotion control in animals and robots: a review," *Neural Networks*, vol. 21, no. 4, pp. 642–653, 2008.

[11] R. Full and D. E. Koditschek, "Templates and anchors: Neuromechanical hypotheses of legged locomotion on land," *Journal of Experimental Biology*, vol. 202, pp. 3325–3332, 1999.

[12] P. Nanua and K. Waldron, "Energy comparison between trot, bound and gallop using a simple model," *Journal of Biomechanical Engineering*, vol. 117, pp. 466–473, 1995.

[13] Z. G. Zhang, Y. Fukuoka, and H. Kimura, "Stable quadrupedal running based spring-loaded two-segment legged on a models," in *Proceedings of the IEEE International Conference on Robotics and Automation*, vol. 3, New Orleans, LA, 2005, pp. 2601–2606.

[14] I. Poulakakis, E. G. Papadopoulos, and M. Buehler, "On the stability of the passive dynamics of quadrupedal running with a bounding gait," *The International Journal of Robotics Research*, vol. 25, no. 7, pp. 669–687, 2006.

[15] Q. Cao and I. Poulakakis, "Passive quadrupedal bounding with a segmented flexible torso," in *Proceedings of the IEEE/RSJ International Conference on Intelligent Robots and Systems*, Vilamoura, Portugal, Oct. 2012, pp. 2484–2489.

[16] Z. Gan and C. Remy, "A passive dynamic quadruped that moves in a large variety of gaits," in *Proceedings of the IEEE/RSJ International Conference on Intelligent Robots and Systems*, Chicago, IN, Sep. 2014, pp. 4876–4881.

[17] Q. Cao and I. Poulakakis, "Passive stability and control of quadrupedal bounding with a flexible torso," in *Proceedings of the IEEE/RSJ International Conference on Intelligent Robots and Systems*, Nov 2013, pp. 6037–6043.

[18] H. K. Khalil, *Nonlinear Systems*, 3rd ed. Upper Saddle River, NJ: Prentice Hall, 2002.

[19] P. A. Parrilo, "Structured semidefinite programs and semialgebraic geometry methods in robustness and optimization," Ph.D. dissertation, California Institute of Technology, 2000.

[20] R. Tedrake, I. R. Manchester, M. Tobenkin, and J. W. Roberts, "LQR-trees: Feedback motion planning via sums-of-squares verification," *The International Journal of Robotics Research*, vol. 29, no. 8, pp. 1038–1052, 2010.